

Nonlinear Spectral Synthesis of Soliton Gas

Andrey A. Gelash

**Institute of Automation and Electrometry SB RAS, Novosibirsk
Skolkovo Institute of Science and Technology, Moscow**

In collaboration with

Dmitry Agafontsev, Skoltech, Moscow

Vladimir Zakharov, Skoltech, Moscow

Gennady El, Northumbria University, Newcastle upon Tyne, UK

Stephane Randoux, University Lille, CNRS, Lille, France

Pierre Suret, University Lille, CNRS, Lille, France

and

A. Tikan, F. Bonnefoy, F. Copie, G. Ducozat, G. Prabhudesai, G. Michel, A. Cazaubiel, E. Falcon

Nonlinear Session – 2020, 14-15 December

Soliton solution of the NLSE

Nonlinear Schrodinger equation (NLSE)

$$i\psi_t + \frac{1}{2}\psi_{xx} + |\psi|^2\psi = 0$$

$$\psi_{1SS}(x, t) = 2\eta \frac{\exp[-2i\xi(x - x_0) - 2i(\xi^2 - \eta^2)t + i\theta]}{ch[2\eta(x - x_0) + 4\xi\eta t]}$$

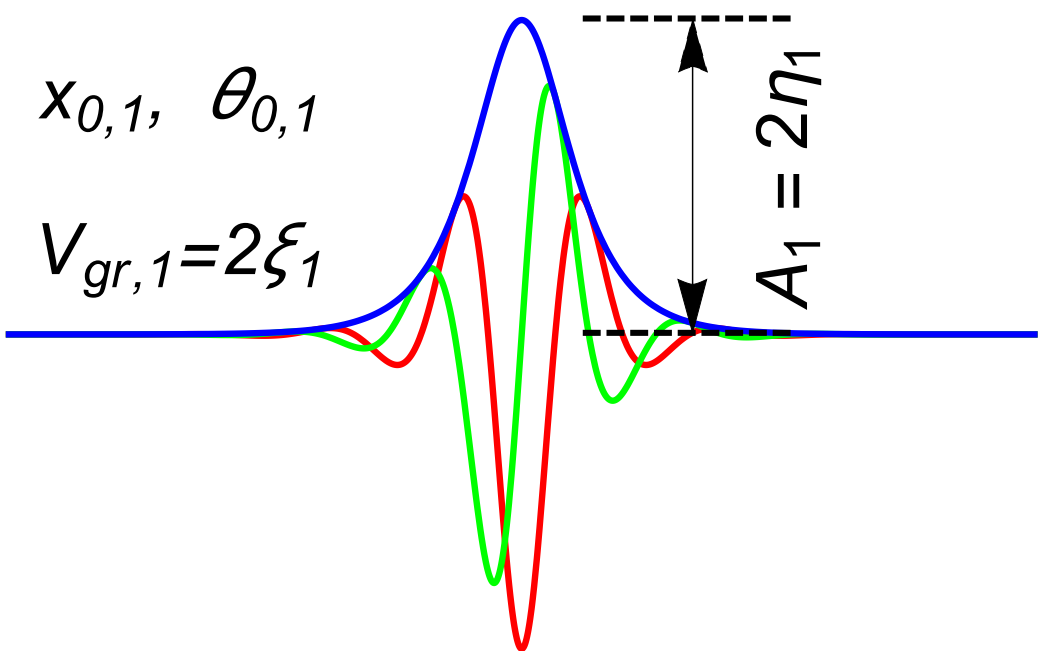
Zakharov-Shabat scattering problem:

$$\Phi_x = \begin{pmatrix} -i\lambda & \psi \\ -\psi^* & i\lambda \end{pmatrix} \Phi = Q\Phi = 0$$

$$\hat{L} = i \begin{pmatrix} 1 & 0 \\ 0 & -1 \end{pmatrix} \frac{\partial}{\partial x} - i \begin{pmatrix} 0 & \psi \\ \psi^* & 0 \end{pmatrix} \quad \hat{L}\Phi = \lambda \Phi$$

Soliton complex discrete eigenvalue:

$$\lambda_j = \xi_j + i\eta_j$$



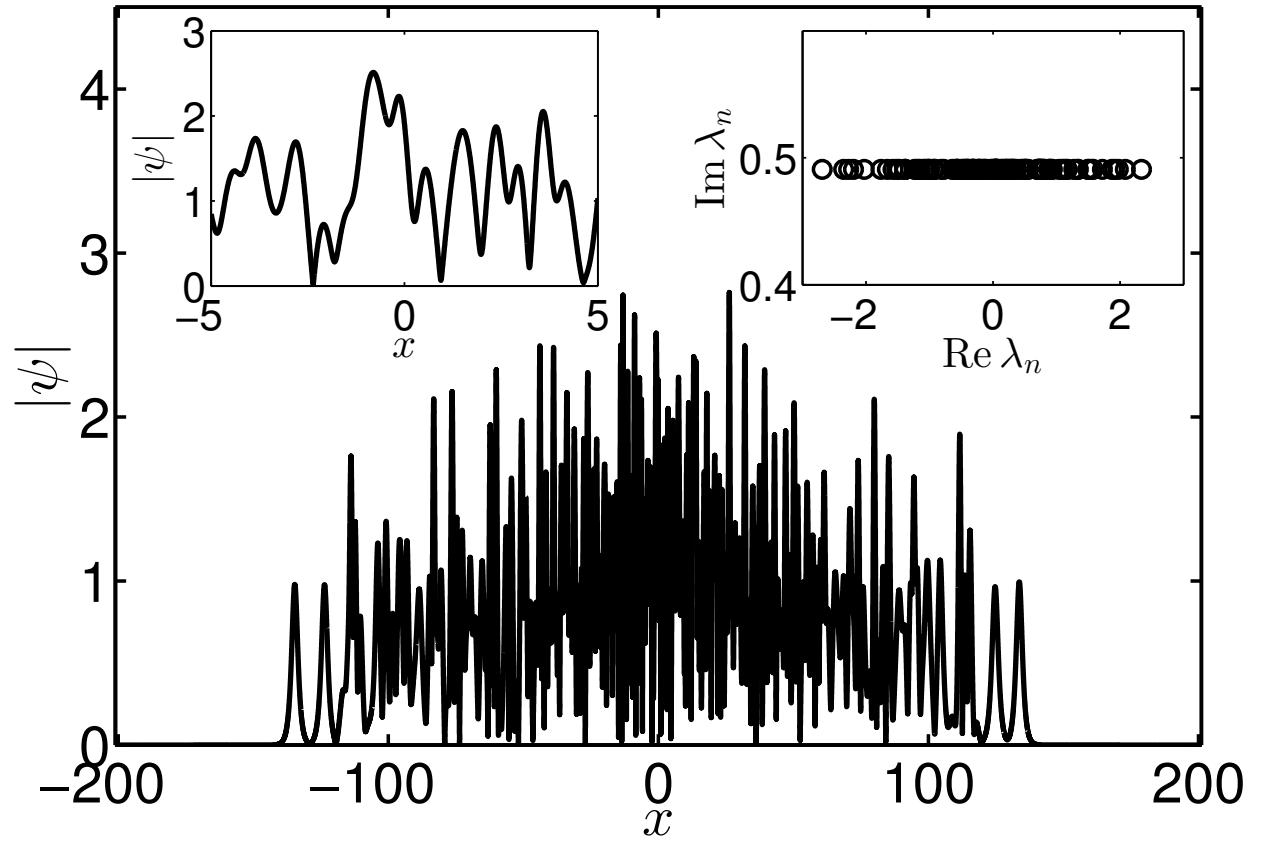
Inverse scattering transform for multi-soliton wave fields

$$\psi_{NSS}(x, t) = \frac{\det \begin{bmatrix} 0 & q_{1,2} & \cdots & q_{n,2} \\ q_{1,1}^* & \frac{(\mathbf{q}_1 \cdot \mathbf{q}_1^*)}{\lambda_1 + \lambda_1^*} & \cdots & \frac{(\mathbf{q}_1 \cdot \mathbf{q}_n^*)}{\lambda_1 + \lambda_n^*} \\ \vdots & \ddots & \ddots & \vdots \\ q_{n,1}^* & \frac{(\mathbf{q}_n \cdot \mathbf{q}_1^*)}{\lambda_n + \lambda_1^*} & \cdots & \frac{(\mathbf{q}_n \cdot \mathbf{q}_n^*)}{\lambda_n + \lambda_n^*} \end{bmatrix}}{\det \begin{bmatrix} (\mathbf{q}_1 \cdot \mathbf{q}_1^*) & \cdots & (\mathbf{q}_1 \cdot \mathbf{q}_n^*) \\ \frac{(\mathbf{q}_1 \cdot \mathbf{q}_1^*)}{\lambda_1 + \lambda_1^*} & \cdots & \frac{(\mathbf{q}_1 \cdot \mathbf{q}_n^*)}{\lambda_1 + \lambda_n^*} \\ \vdots & \ddots & \vdots \\ \frac{(\mathbf{q}_n \cdot \mathbf{q}_1^*)}{\lambda_n + \lambda_1^*} & \cdots & \frac{(\mathbf{q}_n \cdot \mathbf{q}_n^*)}{\lambda_n + \lambda_n^*} \end{bmatrix}}$$

$$\mathbf{q}_j = (\mathbf{e}^{-\phi_j}, \mathbf{e}^{+\phi_j})^T$$

$$\phi_j = -i\lambda_j(x - x_{0,j}) - i\lambda_j^2 t - i\theta_j/2$$

We need high precision !

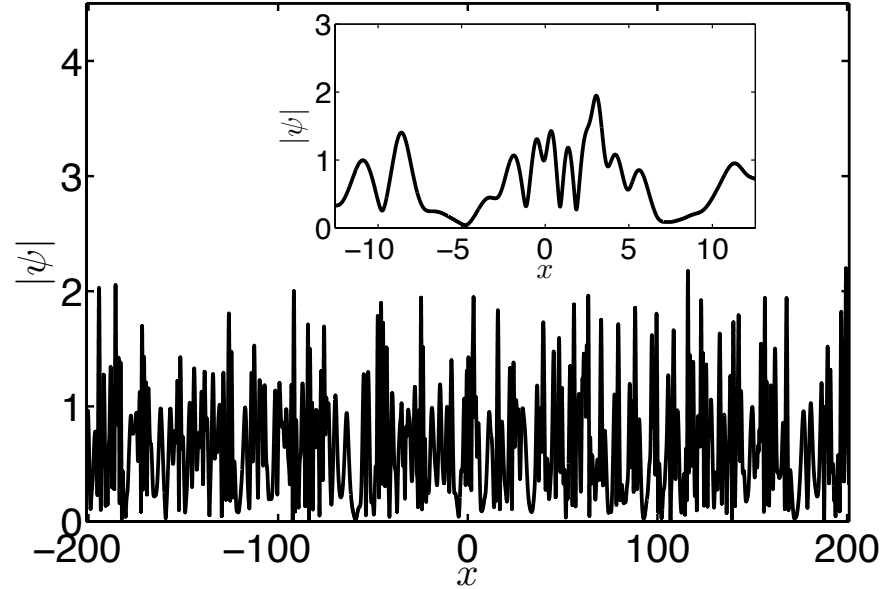
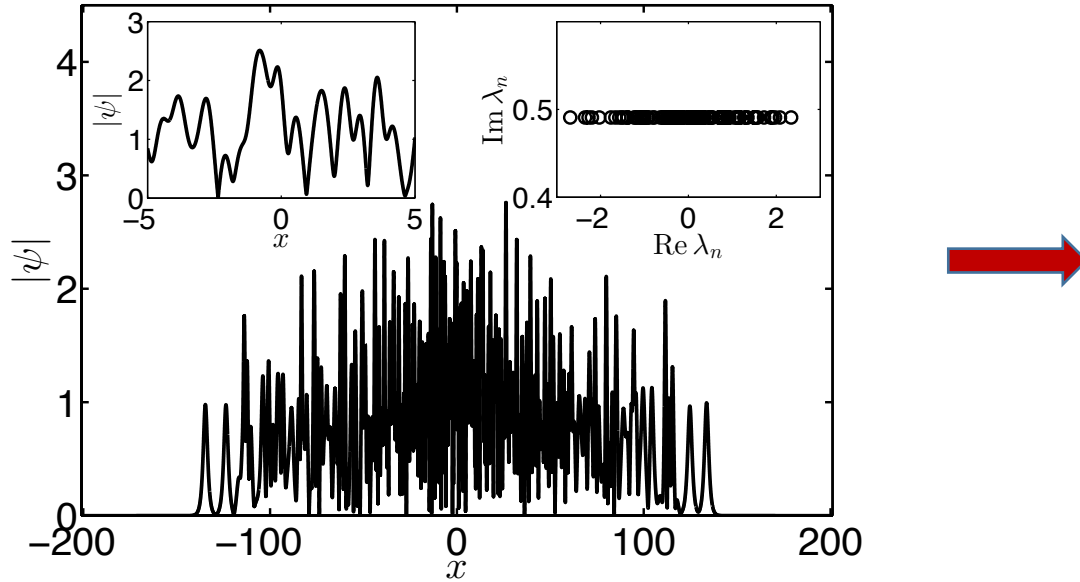


128-soliton solution with random phases

$$x_{0,k} \sim \text{Random}[-2, 2]$$

Statistically homogeneous soliton gas

The question: what is the distribution of $x_{0,k}$ for homogeneous soliton gas??



The same 128-SS as before after stochastization during simulations with periodic boundary conditions (simulation time ~ 100).

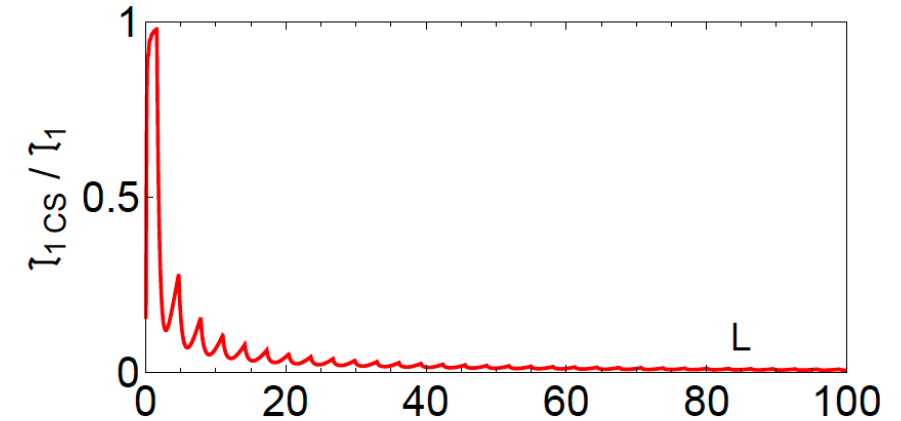
$$\text{Can the mutual soliton shifts be relevant? } \Delta x_{0,k} = \frac{1}{4\eta_k} \ln \left(\frac{|\lambda_j - \lambda_k^*|^2}{|\lambda_j - \lambda_k|^2} \right)$$

The Bohr-Sommerfeld quantization rule for the semiclassical ZS problem:

$$\int \sqrt{|\psi|^2 - \eta_n^2} dx = 2\pi(n - 1/2), \quad \lambda_n = \xi_n + i\eta_n, \quad \xi_n/\eta_n \sim N^{-1/2}$$



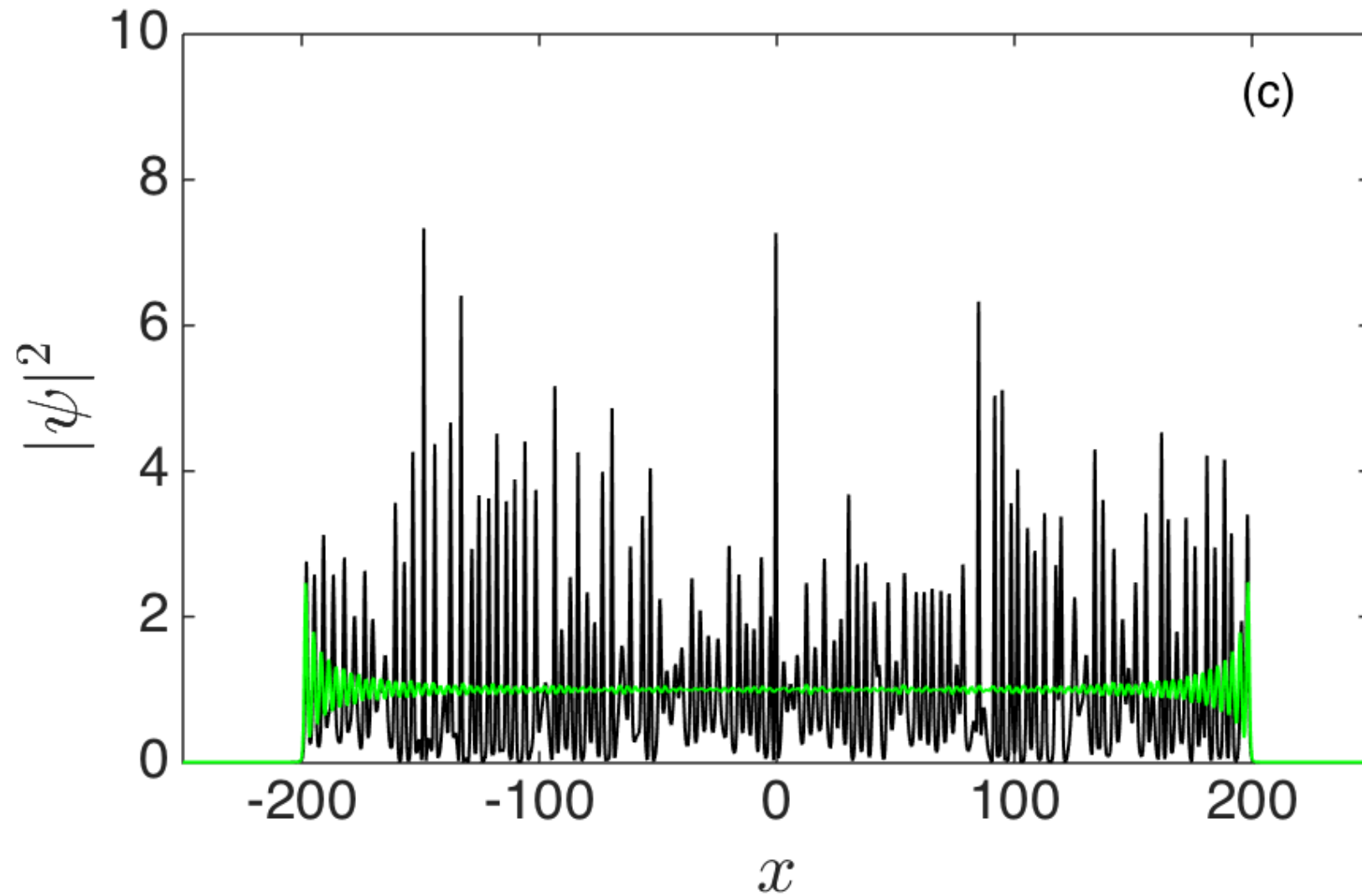
Spatially large region of the condensate,
which we model by a rectangular function.



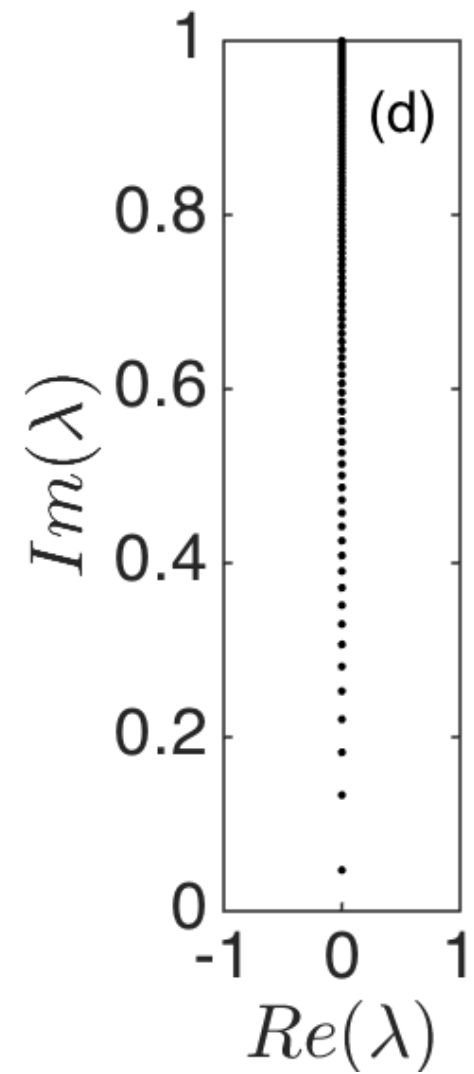
Relative impact of continuous
spectrum to the first integral of the
rectangular wave field.

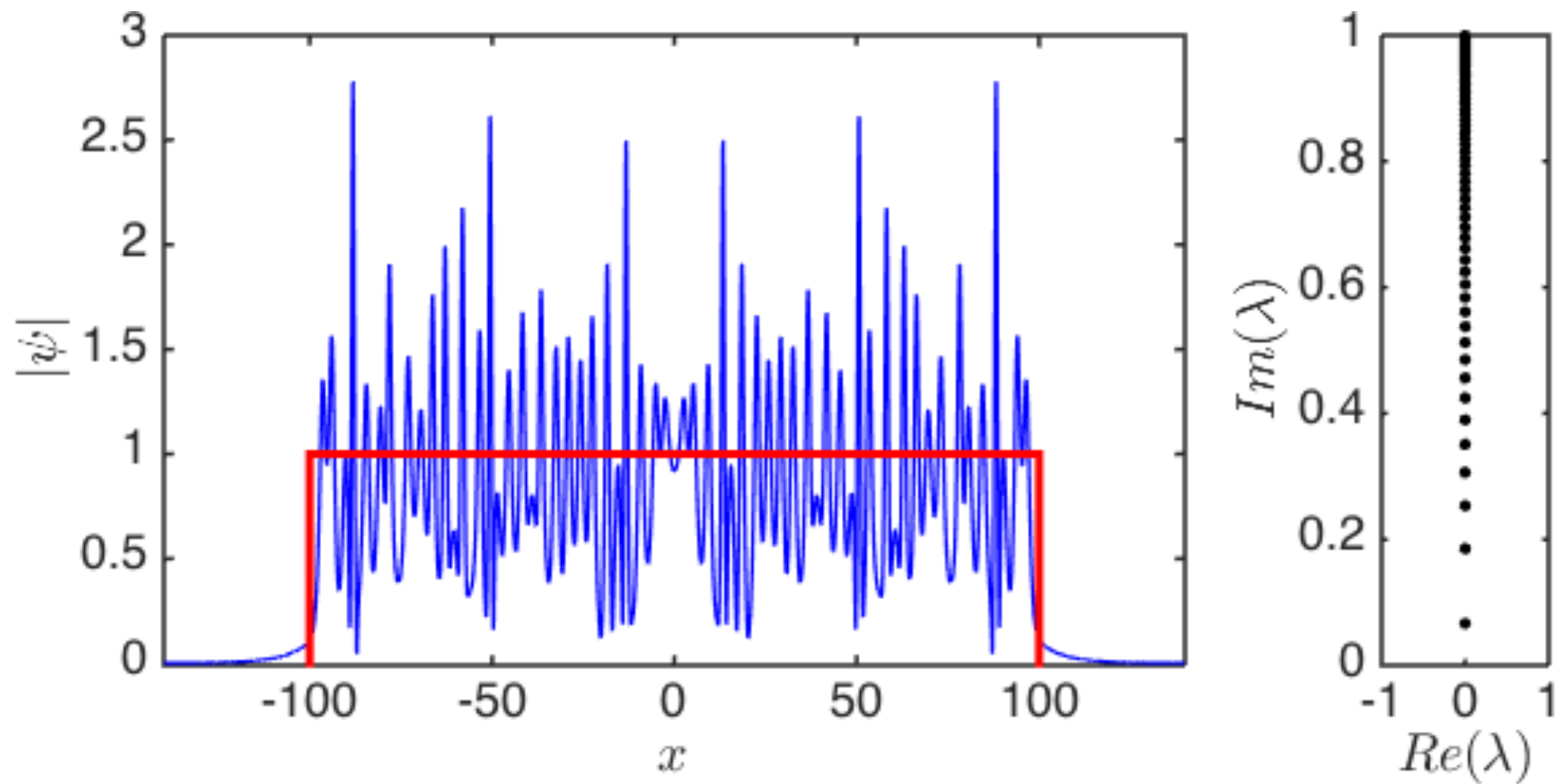
Semiclassical distribution of soliton eigenvalues in the box potential:

$$\lambda_n = i\eta_n = i\sqrt{1 - \left[\frac{\pi(n - 1/2)}{L}\right]^2}, \quad n = 1, 2, \dots, N, \quad N = \text{int}[L/\pi]$$

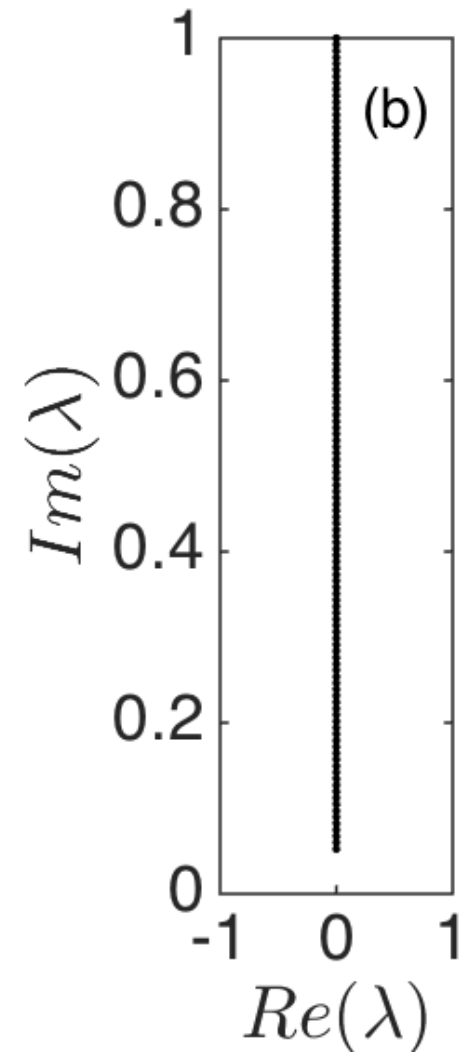
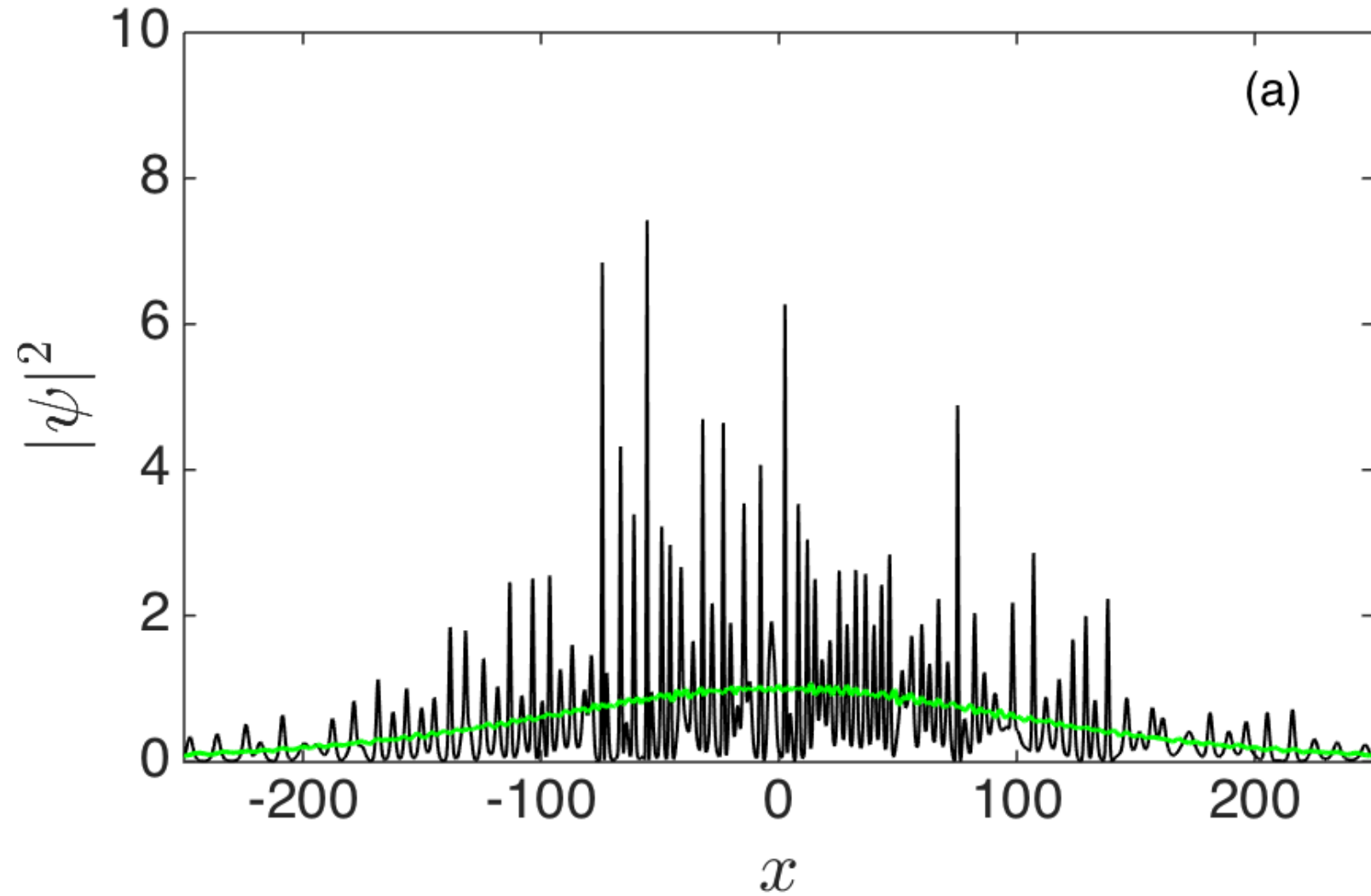


Black lines: 128-soliton solution with random phases, $x_{0,k} \sim \text{Random}[-2,2]$
Green lines: ensemble and time averaged first order moment



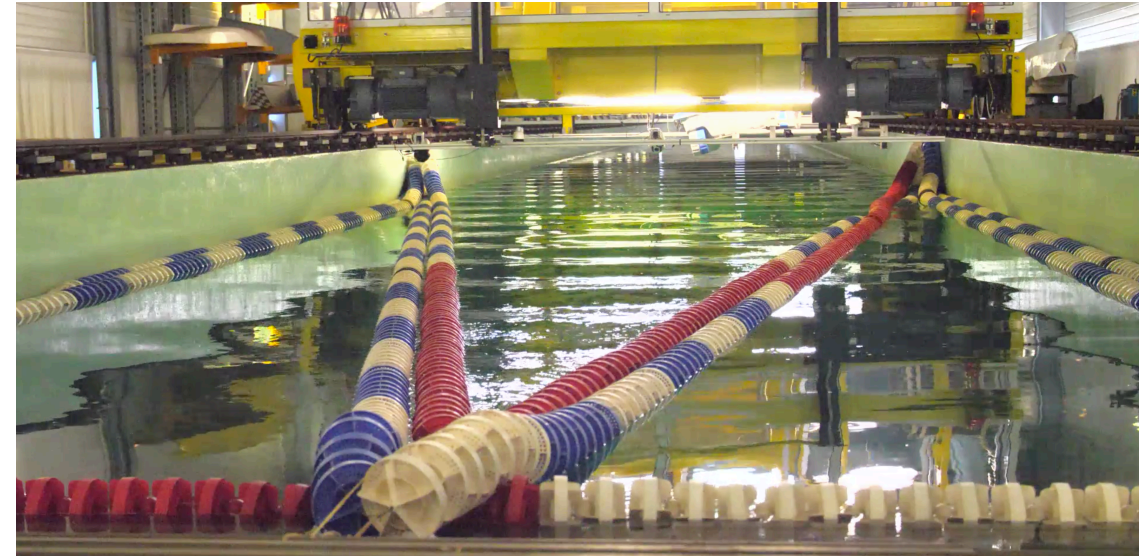


Blue lines: 64-soliton solution with random phases, $x_{0,k} = 0$
Red lines: the corresponding box wave field



Black lines: 128-soliton solution with random phases, $x_{0,k} \sim \text{Random}[-2,2]$
Green lines: ensemble and time averaged first order moment

Water wave tank in Nantes, France. 140 meters, 20 gauges



Integrable dynamics

$$\frac{\partial A}{\partial Z} = i \frac{k_0}{\omega_0^2} \frac{\partial^2 A}{\partial T^2} + i\alpha k_0^3 |A|^2 A$$

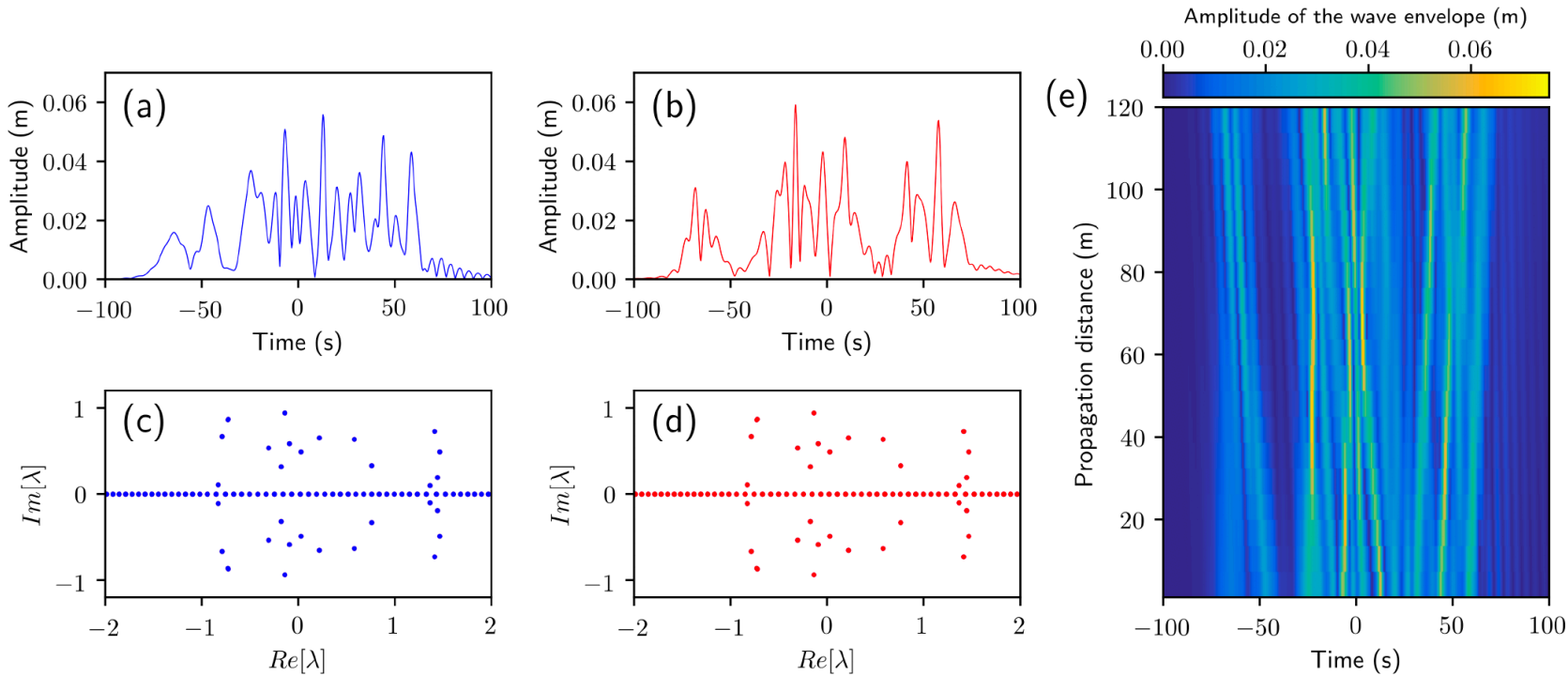


FIG. S1: Integrable dynamics. Numerical simulations of the integrable focusing 1D-NLSE (Eq. (S1) where the last three terms are neglected) for the ensemble of 16 solitons considered in Fig. 1 of the Letter. (a) Modulus $|A(Z_1, T)|$ of the wave envelope at $Z_1 = 6$ m and (c) corresponding discrete IST spectrum (red points). (b) Modulus $|A(Z_{20}, t)|$ of the wave envelope at $Z_{20} = 120$ m and (d) corresponding discrete IST spectrum. (e) Space-time plot showing the nonlinear evolution of the modulus $|A(Z, T)|$ of the wave envelope.

Experimental data

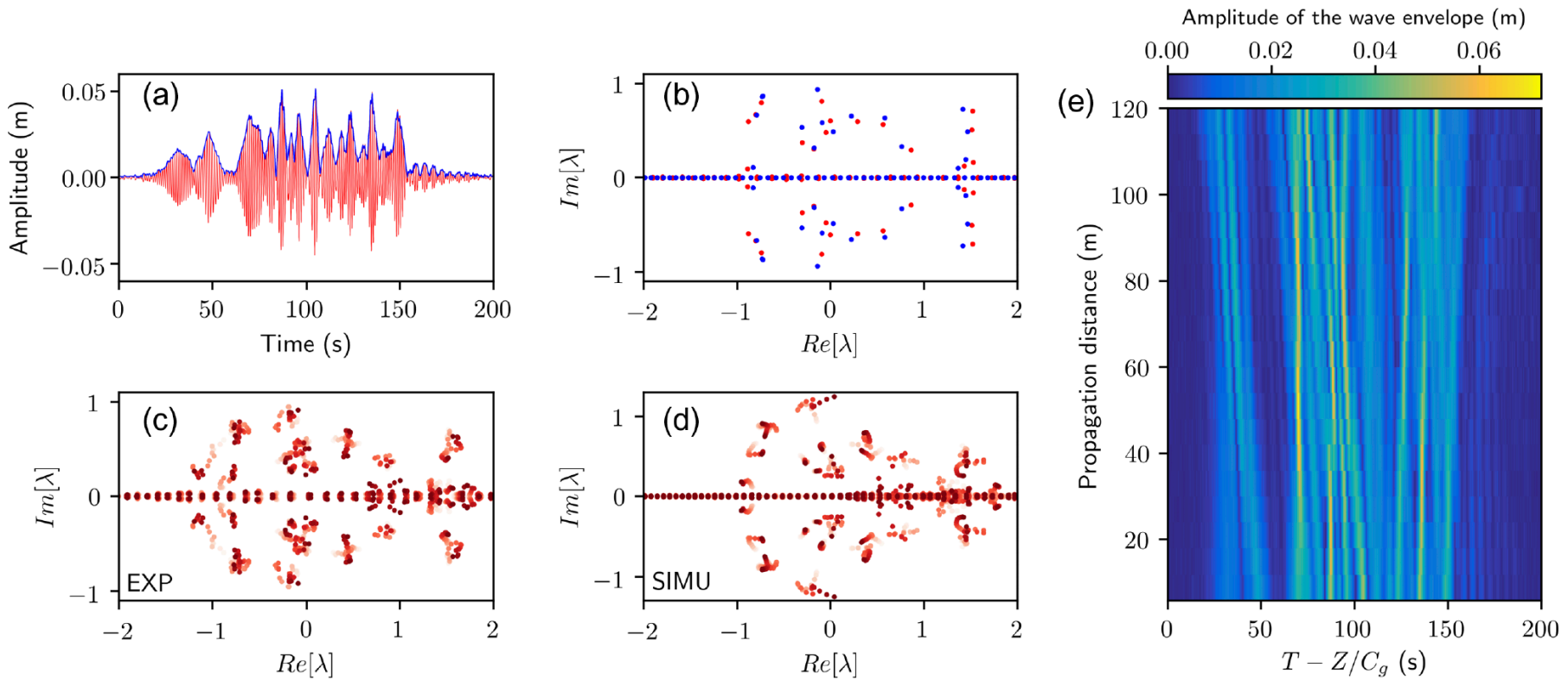


FIG. 1. Ensemble of $N = 16$ solitons propagating in the 1D water tank. (a) Water elevation (red line) and modulus of the wave envelope measured at $Z_1 = 6$ m, close to the wave maker. (b) Blue points represent the discrete IST spectrum of the numerically generated N-SS $\psi_{16}(x, t = 0)$ and red points represent the discrete IST spectrum measured at $Z_1 = 6$ m by using the signal plotted in (a). (c) Space evolution of the discrete IST spectra measured along the tank from $Z_1 = 6$ (light red) to $Z_{20} = 120$ m (dark red). (d) Same as in (c) but obtained from numerical simulations of a modified (not integrable) 1D-NLSE including higher-order effects; see Supplemental Material [53]. (e) Space-time evolution of modulus of the wave envelope recorded by the 20 gauges regularly spaced along the tank. Physical parameters characterizing the experiment are $f_0 = 0.9$ Hz, $k_0 = 3.26$ m $^{-1}$, $\alpha = 0.895$, $L_{\text{NL}} = 210$ m ($\langle |A_0(T)|^2 \rangle = 1.53 \times 10^{-4}$ m 2).

Experimental data

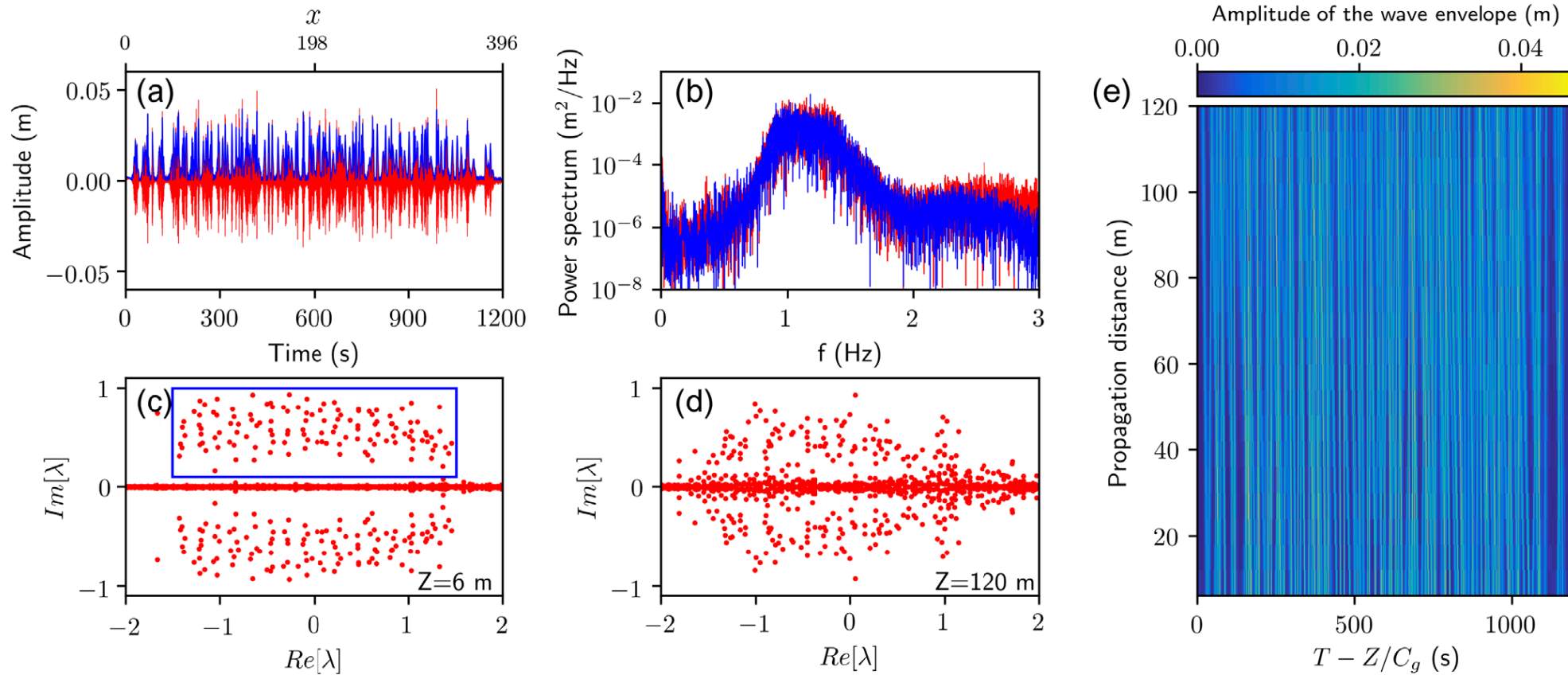


FIG. 2. Gas of $N = 128$ solitons propagating in the 1D water tank. (a) Water elevation (red line) and modulus of the wave envelope measured at $Z_1 = 6$ m, close to the wave maker. (b) Fourier power spectra of wave elevation at $Z_1 = 6$ (blue line) and at $Z_{20} = 120$ m (red line). (c) Discrete IST spectrum measured at $Z_1 = 6$ m. (d) Discrete IST spectrum measured at $Z_{20} = 120$ m. (e) Space-time evolution of modulus of the wave envelope recorded by the 20 gauges regularly spaced along the tank. Physical parameters characterizing the experiment are $f_0 = 1.15$ Hz, $k_0 = 5.32$ m^{-1} , $\alpha = 0.936$, $L_{\text{NL}} = 45$ m ($\langle |A_0(T)|^2 \rangle = 1.58 \times 10^{-4}$ m^2).

Publications:

- [1] A.A. Gelash, and D.S. Agafontsev, Strongly interacting soliton gas and formation of rogue waves, *Phys. Rev. E.*, 2018.
- [2] A. Gelash, D. Agafontsev, V. Zakharov, G. El, S. Randoux and P. Suret,
Bound state soliton gas dynamics underlying the noise-induced modulational instability, *Phys. Rev. Lett.*, 2019.
- [3] P. Suret, A. Tikan, F. Bonnefoy, F. Copie, G. Ducozette, A. Gelash, G. Prabhudesai, G. Michel, A. Cazaubiel, E. Falcon, G. El,
S. Randoux, Nonlinear spectral synthesis of soliton gas in deep-water surface gravity waves.
Phys. Rev. Lett., 2020, accepted.